

Supporting information

Ti₃C₂ MXene as a novel substrate provides rapid differentiation and quantitation of glycan isomers with LDI-MS

*Yuming Jiang,^{ab} Jie Sun,^{ab} Yi Cui,^c Huihui Liu,^{ab} Xiaoyong Zhang,^c Yurong Jiang,^{*d} and Zongxiu Nie,^{*ab}*

- a. Beijing National Laboratory for Molecular Sciences, Key Laboratory for Analytical Chemistry for Living Biosystems, Institute of Chemistry, the Chinese Academy of Sciences, Beijing 100190, China.
- b. University of CAS, Beijing 100049, China.
- c. College of Chemistry, Nanchang University, 999 Xuefu Avenue, Nanchang 330031, China
- d. Department of Optical Engineering, Beijing Institute of Technology, Beijing 100081.

✉Corresponding author: Prof. Yurong Jiang; E-mail: yrkitty@bit.edu.cn Prof. Zongxiu Nie; E-mail: znie@iccas.ac.cn

Supplementary Figures:

Figure S1: TEM image and Layer width distribution of Ti_3C_2 MXene from different batches.

Figure S2: XPS spectrum of C 1s and Ti 2p.

Figure S3: Mass spectra of amino acids, peptides, fatty acids and small metabolites in positive and negative mode with MXene as the substrate.

Figure S4: Mass spectra of maltose ($0.1\mu\text{M}$) with different matrixes in positive mode.

Figure S5: MALDI-LIFT-TOF/TOF spectra of maltose with different matrix.

Figure S6: Relative peak intensity(RPI) of fragment ion pair of maltose as a function of analyte concentration and laser power analyzed by MXene.

Figure S7: MALDI-MS spectra of maltose and maltotriose mixed with alkali metal salt solutions detected by DHB and MXene.

Figure S8: Schematic view and detailed discussion of the model to account for the high ionization efficiency of Ti_3C_2 MXene.

Figure S9: LDI-LIFT-TOF/TOF spectra of two trisaccharides (isomaltotriose and maltotriose) with MXene as substrate.

Figure S10: LDI-LIFT-TOF/TOF spectra of three heptasaccharides with MXene as substrate.

Figure S11: LDI-LIFT-TOF/TOF spectra of disaccharides from different natural product extractions detected by MXene.

Figure S12: Schematic view and detailed discussion of the data analysis and calibration curve plotting of LIFT-TOF/TOF spectra.

Figure S13: Relative quantitation curve of maltose and trehalose.

Figure S14: LDI-LIFT-TOF/TOF spectra of disaccharides in five different kinds of honey.

Figure S15: LDI-LIFT-TOF/TOF spectra of disaccharides in three different kinds of syrup.

Experimental section:

Synthesis and characterization of Ti_3C_2 MXene. The Ti_3SiC_2 ceramic powder was purchased from Forsman Scientific (Beijing) Co., Ltd. The powder (roughly 1 g) was immersed and stirred in 10 mL of a 50% HF aqueous solution (Sinopharm Chemical Reagents Co., Ltd., Shanghai, China) for 3 d at room temperature. After collecting by centrifugation and washing three times with water and ethanol, the precipitate was dispersed in 10 mL of TPAOH (tetrapropylammonium hydroxide 25wt % aqueous solution, J&K Scientific Co., Ltd., Beijing, China) with stirring for 3 d at room temperature. Then, the raw Ti_3C_2 nanosheets were collected by centrifugation and washed three times with ethanol and water to remove the residual TPAOH (Figure 1A) . UV-vis adsorption spectrum was measured by UV-visible light spectrometer [TU1900, Purkinje General Instrument Co., Ltd. (Beijing, China)]. The morphology of Ti_3C_2 MXene was characterized by transmission electron microscopy (TEM, JEM-2010, JEO, Japan) with an accelerating voltage of 120 kV. The chemical composition of 2D Ti_3C_2 MXene was investigated using XPS spectral measurements (ESCALab220i-XL). The zeta potential of different materials were measured at an initial concentration of 8 mg/ml using a Zetasizer (NanoTrac Wave II, Microtrac, USA), the measurements were conducted at room temperature (25 °C).

Materials. Gentiobiose, melibiose, trehalose, laminaribiose, isomaltotriose and maltotriose were purchased from Aladin (Beijing, China). Cellobiose and sucrose were

obtained from J&K (Beijing, China). Isomaltose was purchased from TCI (Tokyo, Japan). Lactose was obtained from ArkPharm (Arlington Heights, IL, U.S.A.). Maltose was purchased from Sigma-Aldrich (St. Louis, MO, U.S.A.). Three heptasaccharide isomers were obtained from Yan Li's group, Institute of Biophysics, Chinese Academy of Sciences. Five different kinds of pure honey samples and three sugar syrups were obtained from Liping Luo's group, Nanchang university. Graphene oxide (GO) and carbon nanotube (CNT) were purchased from Nanjing Xianfeng Nanotechnology Corporation. CHCA and DHB were purchased from Sigma-Aldrich (St. Louis, MO, U.S.A.). The natural products including pure milk, fruits (grape, peach, banana and rockmelon) and cereals (corn, rice, wheat, yam and mung) were purchased from Jintai supermarket in Haidian district, Beijing. The water used was prepared using a Milli-Q water purification system from Millipore (Milford, MA, U.S.A.).

Sample Preparation for MALDI-TOF MS Analysis. The Ti_3C_2 MXene was dissolved in water at the concentration of 2 mg/ml. Graphene oxide (GO) and carbon nanotube (CNT) were dissolved in water at the concentration of 1 mg/ml. CHCA and DHB were prepared as a saturated solution in CH_3CN /water (2:1, v/v) containing 0.1% trifluoroacetic acid (TFA). nine disaccharides, two trisaccharides and three heptasaccharides were dissolved in water at the concentration of 0.2mM. The natural products were extracted by a mixture solution of methanol/water(1:1, v/v) with two hours. Then equal volumes (1 μL) of Ti_3C_2 MXene solution and analyte was mixed and 1 μL of resulting solution was deposited on the MALDI target plate and air-dried for further MS

or MS/MS analysis.

MALDI-TOF MS Analysis. MALDI-TOF MS analysis was performed on a Bruker Ultraflextreme mass spectrometer (Bruker Daltonics, Germany) equipped with a 355 nm smartbeam Nd:YAG pulsed laser. PEG 600 and oligosaccharides were used for negative and positive ion mode mass calibration, respectively. The laser power energy was adjusted between 0% and 100% to provide laser pulse energy between 0 and 100 μJ per pulse. The mass spectra were typically recorded at an accelerating voltage of 19 kV, a reflection voltage of 20 kV, and with a laser pulse energy of 60 μJ . Unless otherwise stated, each mass spectrum was acquired as an average of 200 laser shots at 500 Hz frequency.

MALDI-LIFT-TOF/TOF MS Analysis. MALDI mass spectra and LIFT spectra were acquired in positive mode using a reflectron geometry MALDI-TOF/TOF (Ultraflextreme, Bruker Daltonics, Germany) equipped with a 355 nm and 2k Hz solid state Nd:YAG Smart Beam laser. The laser power was set at 35% while conducting LIFT. The mass selection window was set at 2 Da. The mass spectrum was summed up by 1000 shots at a laser repetition rate of 200 Hz and analyzed by flexAnalysis (Bruker Daltonics, Germany). The average intensity and standard deviation of six measurements were used to build the calibration curve.

Supplementary figures

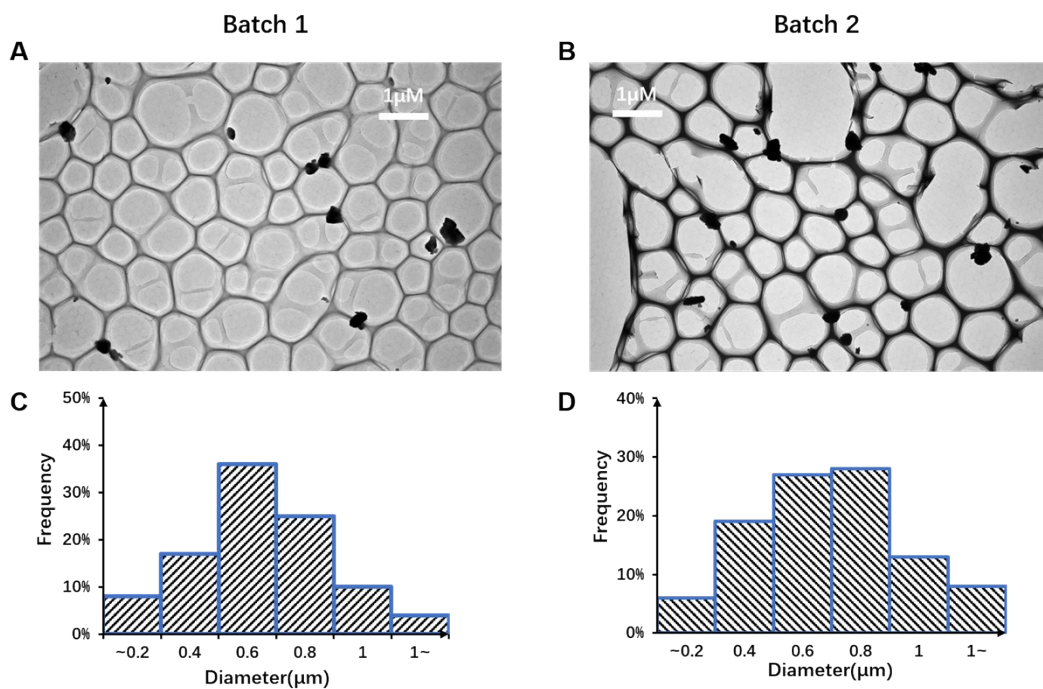


Figure S1. (A) TEM image of Ti_3C_2 MXene from batch 1. (B) TEM image of Ti_3C_2 MXene from batch 2. (C) Layer width distribution of the Ti_3C_2 MXene from batch 1. (D) Layer width distribution of the Ti_3C_2 MXene from batch 2.

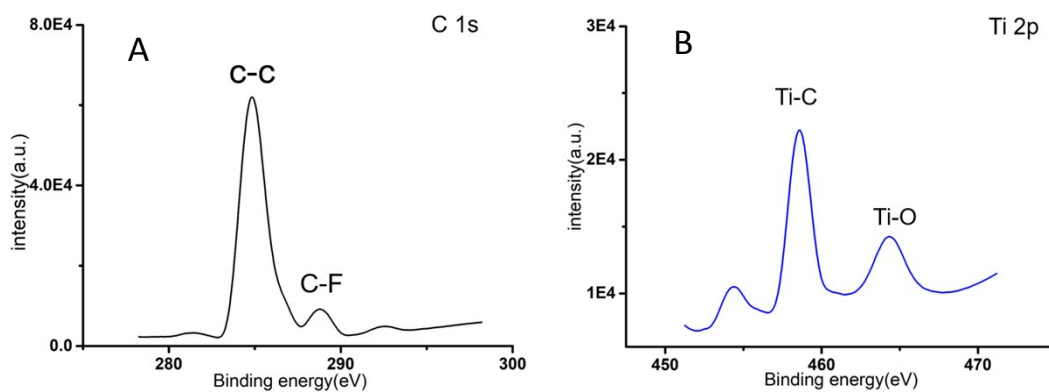


Figure S2. (A) XPS spectrum of C 1s, (B) XPS spectrum of Ti 2p.

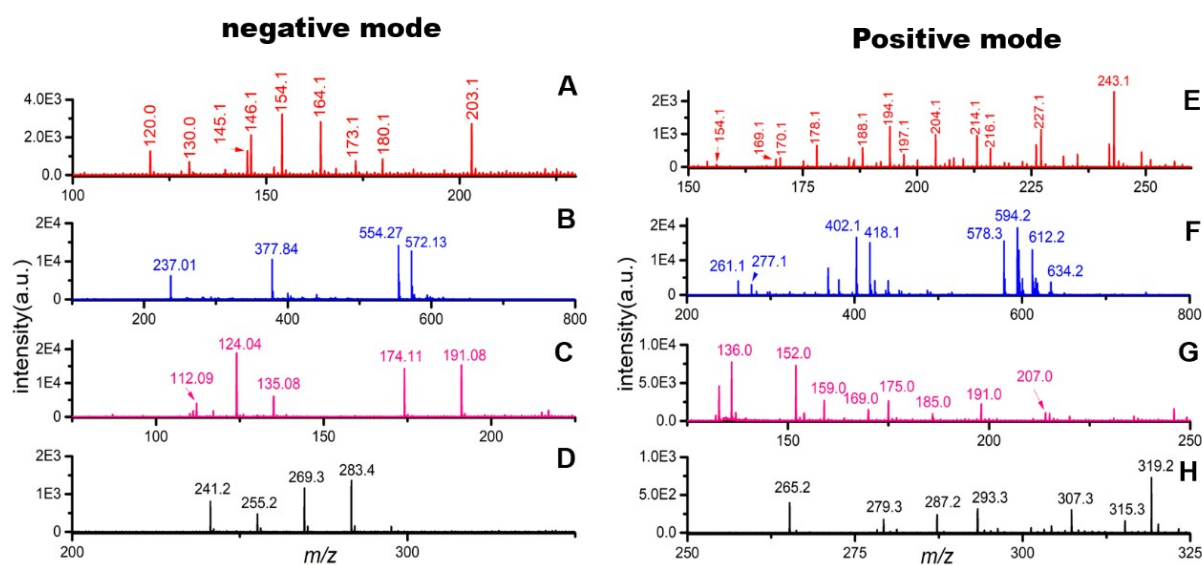


Figure S3. Mass spectra of a solution include nine amino acids Cys (MW121.1), Leu (MW 131.1), Lys(MW 146.1), Glu (MW 147.0), His (MW 155.1), Phe(MW 165.1), Arg (MW 174.1), Tyr (MW 181.1), and Trp (MW 204.1) in (A) negative mode and (E) positive mode, (B) a solution contain four peptides Gly-Tyr (MW 237.95), Val-Tyr-Val (MW 378.71), Tyr-Gly-Gly-Phe-Leu (MW 555.16) and Asp-Arg-Val-Tyr-Ile-His-Pro-Phe (MW 573.08) in negative mode and (F) positive mode (C) a solution contain five small metabolites including creatinine (MW 113.09), taurine (MW 125.01), hypoxanthine riboside (MW136.04), N-acetyl aspartic acid (MW 175.07), and citric acid (MW 192.06) in negative mode and (G) positive mode. (D) a solution contain four fatty acids pentadecanoic acid(MW 242.40), hexadecanoic acid(MW 256.43), heptadecanoic acid (MW 270.45), octadecanoic acid (MW 284.48) and (H) positive mode. The amount of each analyte is 500 pmol.

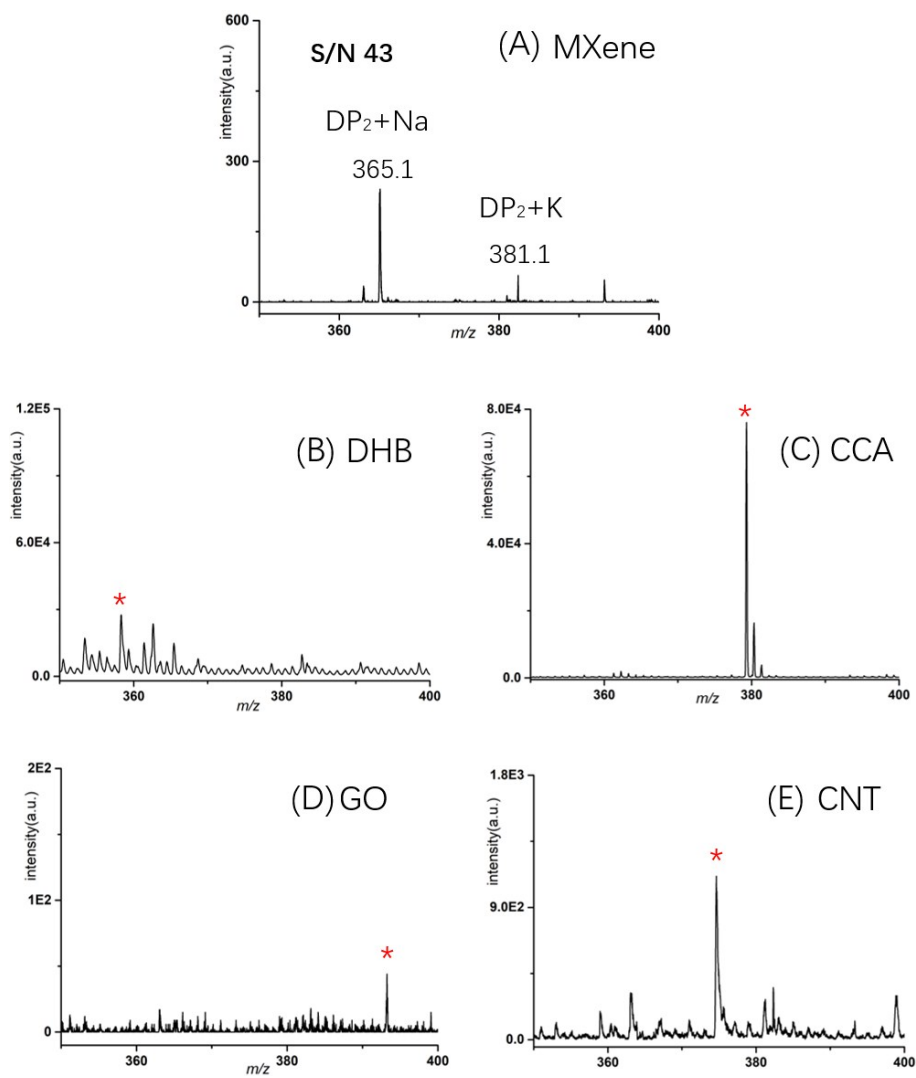


Figure S4. MALDI-TOF mass spectra of maltose (m/z 365.1, $[M+Na]^+$) with different matrix (A) Ti_3C_2 MXene, (B) DHB, (C) CHCA, (D) Graphene oxide, (E) Carbon nanotube. The amount of maltose is 50 fmol. The concentration of maltose is 0.1 μ M. Only MXene can detect maltose signal, with a signal-to-noise ratio of 43. The red asterisk represents the interference peak.

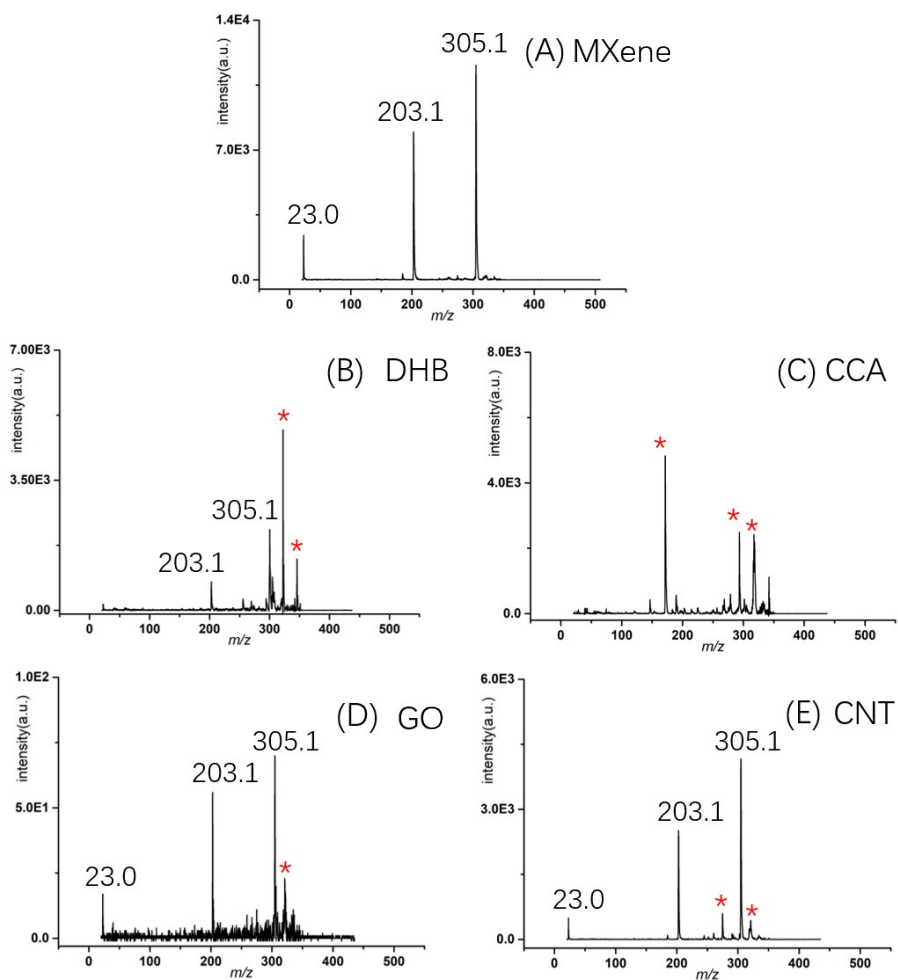


Figure S5. MALDI-LIFT-TOF/TOF spectra of maltose (m/z 365.1, $[M+Na]^+$) of different matrix (A)MXene (B) DHB.(C) CHCA. The amount of maltose is 25 pmol. The concentration of maltose is 0.05 mM.

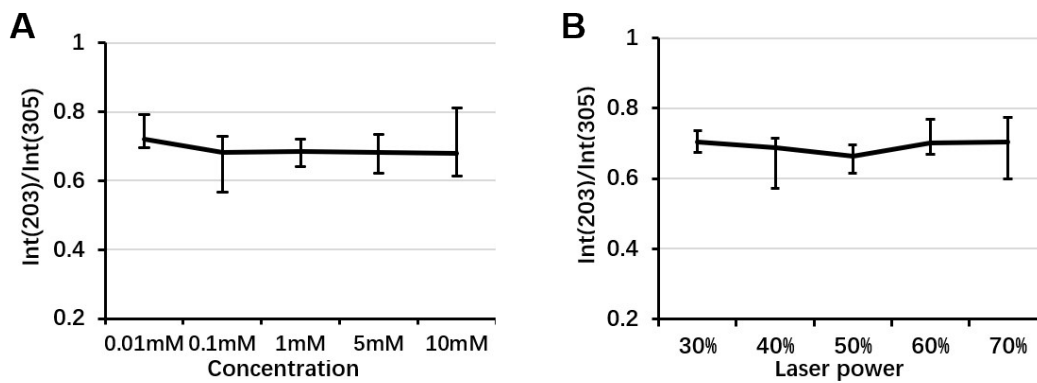


Figure S6. (A) Relative peak intensity(RPI) of fragment ion pair (m/z 203.0/305.1) of maltose as a function of analyte concentration analyzed by MXene. (D) Relative peak intensity(RPI) of fragment ion pair (m/z 203.0/305.1) of maltose as a function of laser power analyzed by MXene.

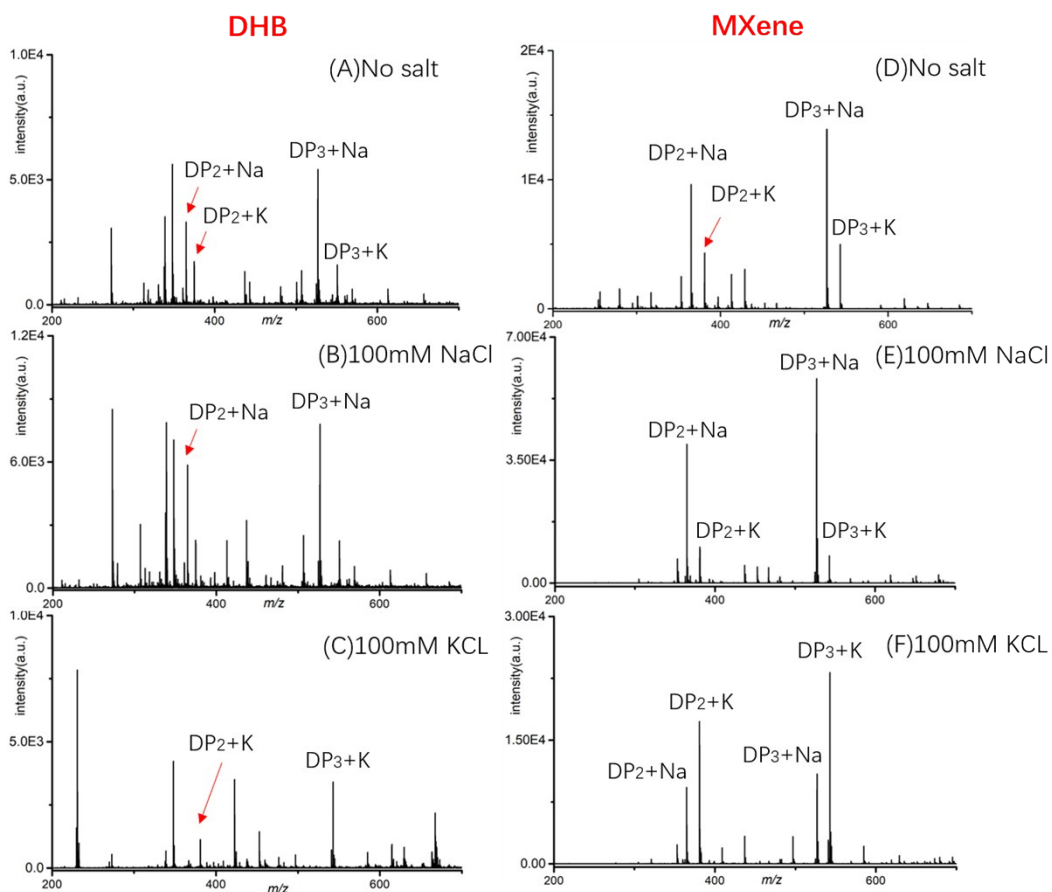


Figure S7. MALDI-MS spectra of maltose and maltotriose mixed with alkali metal salt solutions detected by DHB and MXene. (A) DHB with no salt addition (B) DHB with 100mM NaCl addition (C) DHB with 100mM KCl addition (D) MXene with no salt addition (E) MXene with 100mM NaCl addition (F) MXene with 100mM KCl addition.

Discussion: As we can see in Figure S7, for normal situation, the intensity of sodium-adduct ion is higher than potassium-adduct ion in both matrixes. However, with extra addition of sodium, the intensity of sodium-adduct oligosaccharide ion significantly increased in both matrixes and the ratio between sodium-adduct and potassium-adduct increased (>3). Similarly, with extra addition of potassium, the intensity of potassium-adduct oligosaccharide ion significantly increased in both matrixes and the ratio between sodium-adduct and potassium-adduct is reversed (<0.5). These results proved that alkali metal-adducted ion is the major channel for the formation of the carbohydrate precursor ion, and the concentration of alkali metal ion is crucial to the formation of the specific alkali metal-adduct carbohydrate precursor ion.

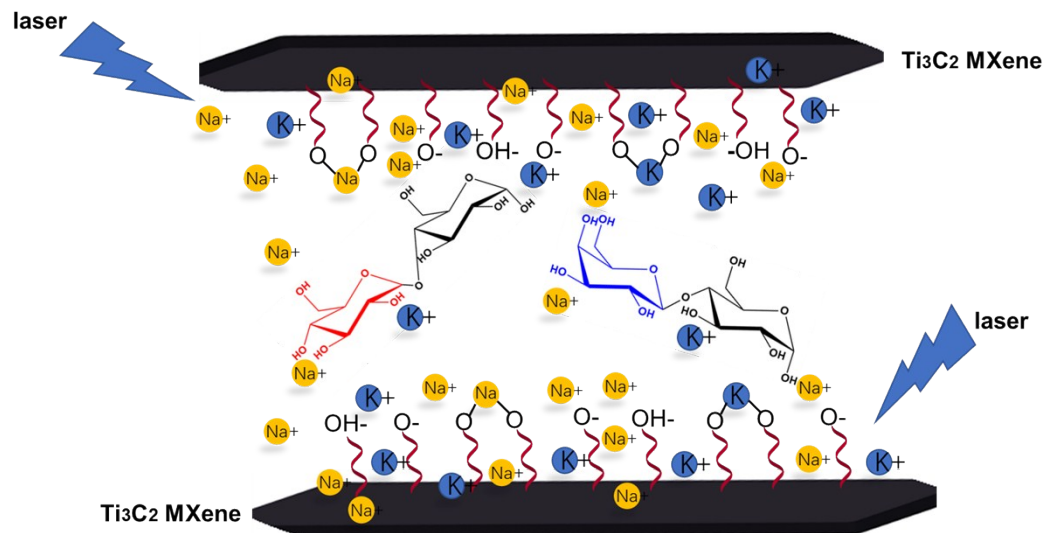


Figure S8. Schematic view of the model to account for the high ionization efficiency of Ti_3C_2 MXene.

Discussion:

Formation of ions from molecules in the LDI process involves the contribution of two steps: one is desorption, turning condensed phase molecules into gas-phase molecules; the other is ionization, transferring gas-phase molecules into ions (these two steps may take place simultaneously).^{1,2}

a) For the desorption step. We designed an experiment to gauge its desorption efficiency. A preformed ion tetraphenylborate was used to test the desorption efficiency. As the tetraphenylborate is already negatively charged, so its MS signal intensity can be used to gauge the desorption efficiency of the matrixes used. We compared three different matrixes including MXene, graphene oxide, DHB and a control group with no matrix. The results clearly showed a strongest intensity can be obtained with MXene as the matrix (Figure 2C), which proved the superior desorption efficiency of Ti_3C_2 MXene.

b) For the ionization step. The composition of ions here we applied for glycan analysis are mainly sodium adduct $[\text{M}+\text{Na}]^+$ and potassium adduct $[\text{M}+\text{K}]^+$ ions, and the formation of sodium adduct $[\text{M}+\text{Na}]^+$ and potassium adduct $[\text{M}+\text{K}]^+$ ions are highly related to the amount of sodium and potassium in the solution (proved in Figure S7). As been reported before, the Ti_3C_2 MXene can be

used for adsorption of metal ions in water through electrostatic attraction³ and chemical interactions⁴. For electrostatic attraction, we tested the zeta potential of MXene in distilled water and compared with other materials like graphene oxide and carbon nanotube. Results proved that the surface of Ti_3C_2 MXene was negatively charged and the zeta potential was the lowest among three materials (Figure 2D), which proved the electrostatic attraction between Ti_3C_2 MXene and metal ions. For chemical interactions, the XPS result (Figure S1) proved the successfully introduction of abundant highly active surface sites (-O and -OH), which can be used to trap metal ions through hydroxyl potential traps, forming strong bonds between metal ions and oxygen atoms (hydroxyls losing H atoms)⁵. These two pathways allow sodium and potassium accumulate on the surface of MXene.

Based on above, we proposed a model to explain how Ti_3C_2 MXene can enhance ionization efficiency in LDI-MS. firstly, based on the electrostatic attraction of negatively charged surface (proved in Figure 2D) and chemical interactions between terminal groups (-OH, -O) and metal ions, a large number of metal ions like sodium and potassium will be adsorbed on the surface of the Ti_3C_2 material. As we know, The alkali metal-adducted ion has been reported to be the major channel for the formation of the carbohydrate precursor ion, and the concentration of alkali metal ions is crucial to the formation of alkali metal-adduct carbohydrate precursor ion (proved in Figure S7), so we believe the metal ion rich surface of Ti_3C_2 MXene will be a huge boost to the eventual formation of sodium-adduct oligosaccharide ions. What's more, owing to the large specific surface area and layer structure of 2D Ti_3C_2 MXene, a sandwich-like structure will formed and provided more opportunities for interactions between oligosaccharide and alkali metal ions (Figure S8). Finally, after air dried and laser irradiation, owing to the good desorption efficiency and thermal effect of Ti_3C_2 MXene (proved in Figure 2C), the Ti_3C_2 MXene absorbs, converts and pools the laser energy, causing the entire “sandwich” structure to “heat up”. The alkali metal-adduct oligosaccharide molecule absorbs this heat and subsequently desorbs to the gaseous plume.

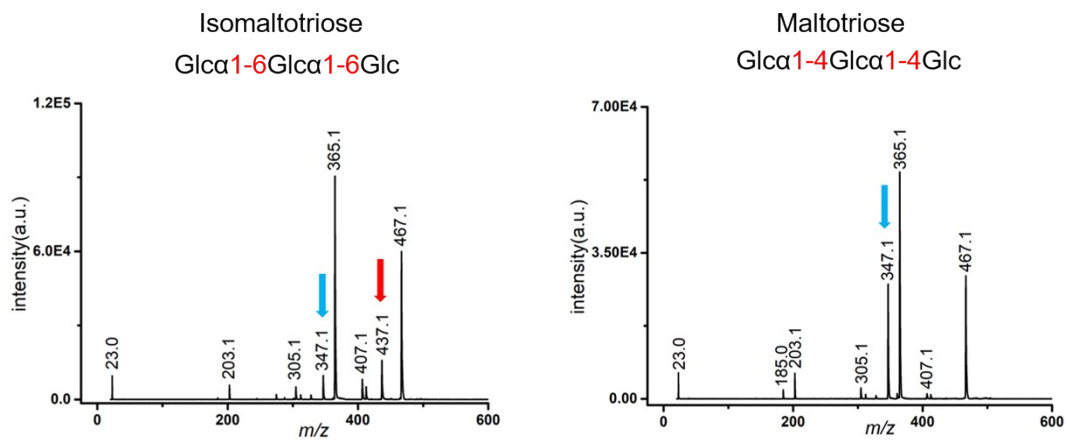


Figure S9. LDI-LIFT-TOF/TOF spectra of the precursor ions $[M + Na]^+$ (m/z 527.2) obtained from two trisaccharides (isomaltotriose and maltotriose) with MXene as substrate. The amount of each analyte is 100 pmol.

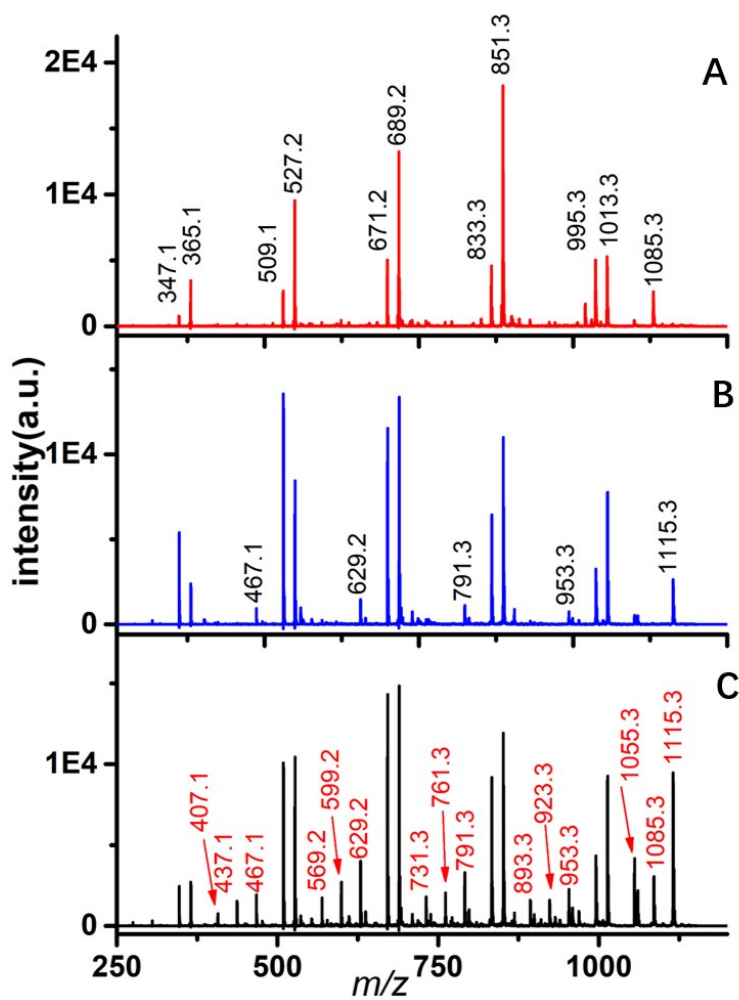


Figure S10. LDI-LIFT-TOF/TOF spectra of the precursor ions $[M+Na]^+$ (m/z 1175.4) obtained from three hepta-saccharides:(A)Glc α 1-3Glc α 1-3Glc α 1-3Glc α 1-3Glc α 1-3Glc α 1-3Glc; (B)Glc α 1-4Glc α 1-4Glc α 1-4Glc α 1-4Glc α 1-4Glc α 1-4Glc; (C)Glc α 1-6Glc α 1-6Glc α 1-6Glc α 1-6Glc α 1-6Glc α 1-6Glc;with MXene as matrix, respectively. The amount of each analyte is 100 pmol.

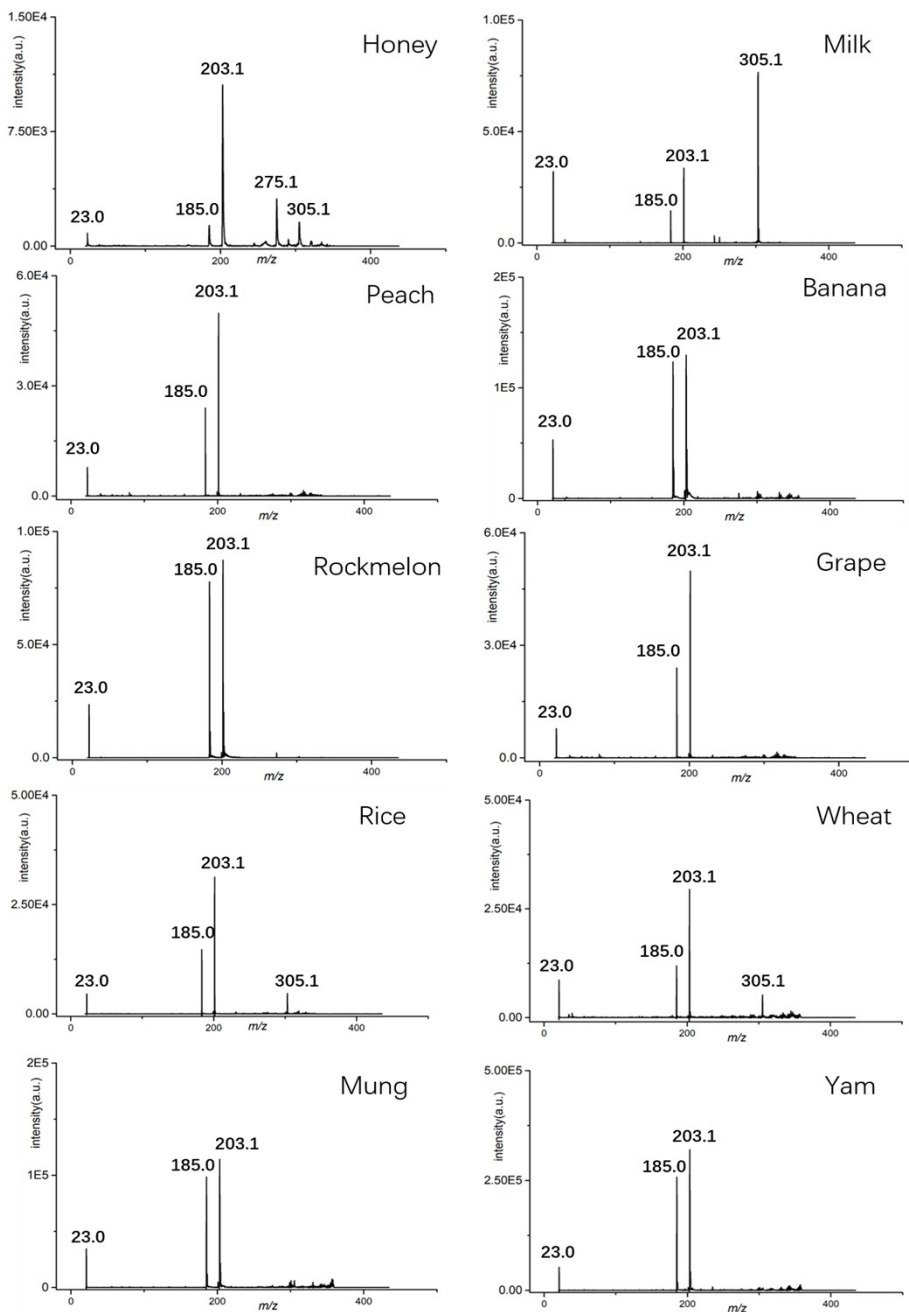


Figure S11. LDI-LIFT-TOF/TOF spectra of disaccharides ($[M + Na]^+$ m/z 365.1) obtained from different natural product extractions including honey, milk, peach, banana, rockmelon, grape, rice, wheat, mung and yam. The natural products were extracted by a mixture solution of methanol/water(1:1, v/v) with two hours.

Disussion: The results proved that the Ti_3C_2 MXene can also be used for real sample testing. As we

can see from the typical LIFT-MS/MS spectrum of disaccharides, owing to the different composition of disaccharide isomers in different natural products, the fragment profiles of different natural products exhibit their uniqueness. For example, the fragment profile of disaccharide in milk showed its main composition is lactose, for fruits including peach, banana, rockmelon and grape is sucrose (strong m/z 185.0 and 203.1, no other peaks, similar to the fragment profile of pure sucrose sample), for cereals like rice and wheat is sucrose and maltose (strong intensity and appropriate ratio of m/z 185.0 and 203.1, relatively weak intensity of m/z 305.1 and no other cross-ring cleavage fragments). These results indicated that the method we proposed can also be used for glycan isomer differentiation in real samples.

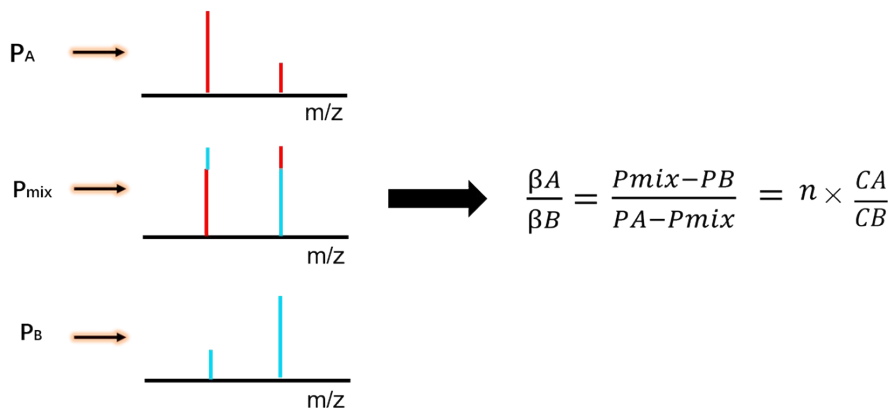


Figure S12. Schematic view of the data analysis and calibration curve plotting of LIFT-TOF/TOF spectra.

Discussion:

The method we proposed here is briefly described as below^{6, 7}:

Just like the schematic view we showed above, every glycan isomer has its own specific fragment pattern, and the ratio of intensity between different fragment ions are stable in LIFT-MS/MS mode when detected by MXene. Therefore, when two isomers are mixed, there is a correlation of the fragment profile between the mixture and the two isomers involved in the mixture.

Firstly, we selected two fragment ions as the special ion pair. Here, it is usually to choose two peaks with large difference in intensity ratio, which helps to reduce the error. Assuming that P_{mix} represents the intensity ratio of two selected specific fragment ions from the mixture, P_A and P_B represent the intensity ratios of two selected specific fragment ions from isomer A and isomer B, respectively. And the β_A and β_B represent fractions of isomer A and B in the gas phase. Then we can get an equation:

$$P_{\text{mix}} = P_A\beta_A + P_B\beta_B \quad (1)$$

In this equation, the value of P_{mix} , P_A and P_B are known, which can be directly obtained from the LIFT spectra. So the ratio of β_A/β_B can be calculated. However, the β_A and β_B can not directly comparable to their concentrations (C_A and C_B) in solution due to the different efficiencies of ionization and fragmentation. So a relationship between β and C values was assumed:

$$\beta_A/\beta_B = n \times (C_A/C_B) \quad (2)$$

Where the C values represent their prepared concentrations in solution. The ratio of β_A to β_B are calculated from the intensity ratios P of selected fragment ions. Then we can construct the calibration curve by plotting the ratio of β values against that of C values.

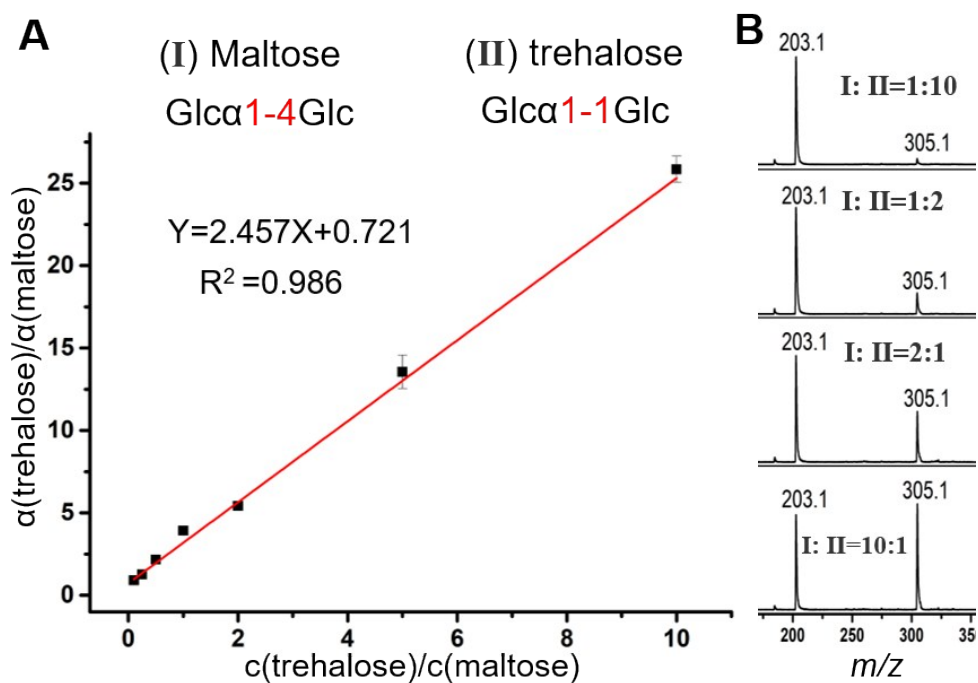


Figure S13. Calibration curve of maltose and trehalose, constructed with fragment ions m/z 203.1 and 305.1: (A) The calibration curve. (B) The diagnostic product ion pair used to construct the calibration curve, m/z 203.1 and 305.1, in various mixtures with different ratio of disaccharides isomers (molar ratios of maltose and trehalose were 1:10, 1:2, 2:1, 10:1).

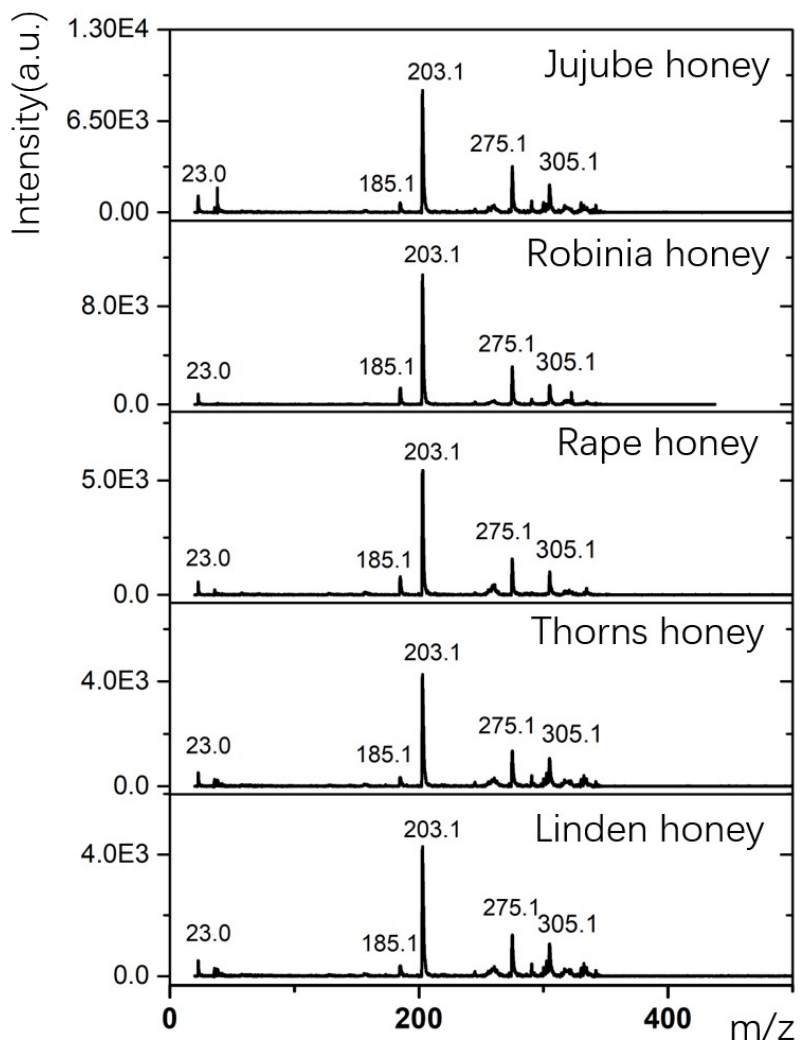


Figure S14. LDI-LIFT-TOF/TOF spectra of disaccharides ($[M + Na]^+$ m/z 365.1) in five different kinds of honey (jujube, robinia, rape, thorns, linden) with MXene as substrate. The amount of each analyte is 5 mg/ml.

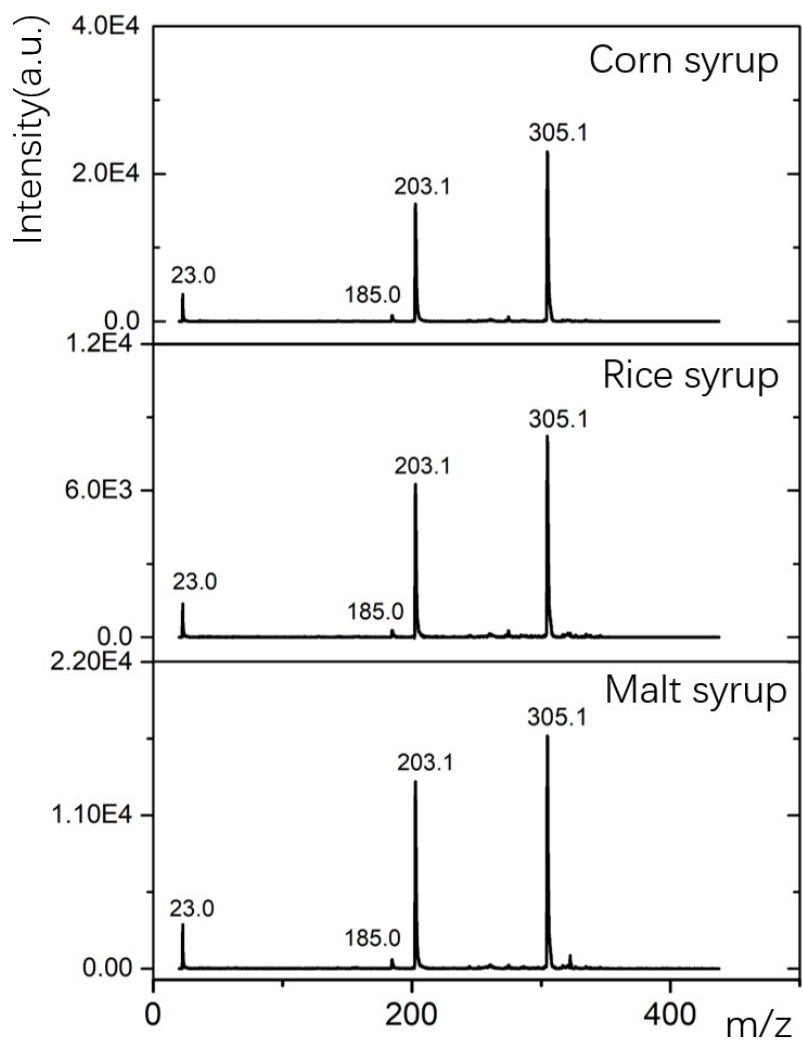


Figure S15. LDI-LIFT-TOF/TOF spectra of disaccharides ($[M + Na]^+$ m/z 365.1) in three different kinds of syrup (corn, rice, malt) with MXene as substrate. The amount of each analyte is 5 mg/ml.

Supplementary Reference:

1. R. A. Picca, C. D. Calvano, N. Cioffi and F. Palmisano, *Nanomaterials*, 2017, **7**.
2. K.-M. Ng, S.-L. Chau, H.-W. Tang, X.-G. Wei, K.-C. Lau, F. Ye and A. M.-C. Ng, *The Journal of Physical Chemistry C*, 2015, **119**, 23708-23720.
3. A. Shahzad, K. Rasool, W. Miran, M. Nawaz, J. Jang, K. A. Mahmoud and D. S. Lee, *ACS Sustainable Chemistry & Engineering*, 2017, **5**, 11481-11488.
4. Q. Peng, J. Guo, Q. Zhang, J. Xiang, B. Liu, A. Zhou, R. Liu and Y. Tian, *Journal of the American Chemical Society*, 2014, **136**, 4113-4116.
5. J. Guo, Q. Peng, H. Fu, G. Zou and Q. Zhang, *The Journal of Physical Chemistry C*, 2015, **119**, 20923-20930.
6. H. H. L. Lee, J. W. Lee, Y. Jang, Y. H. Ko, K. Kim and H. I. Kim, *Angewandte Chemie International Edition*, 2016, **55**, 8249-8253.
7. L. Zhan, X. Xie, Y. Li, H. Liu, C. Xiong and Z. Nie, *Analytical chemistry*, 2018, **90**, 1525-1530.